ACS OMEGA

http://pubs.acs.org/journal/acsodf

Article

Antioxidant Behavior Affected by Polarity in the Olive Oil: Experimental and Molecular Simulation Investigations

Jie Tang, Guohua You, Lu Ruan, Yi Lu, Bianying Wen,* and Sizhu Wu*

Cite This: *ACS Omega* 2021, 6, 7119−7126

Read Online

ACCESS | Metrics & More | Article Recommendations

ABSTRACT: Natural antioxidants are essential potential sources for protecting the oxidation of food oils. However, until now, the mechanisms are still not very clear, especially from the quantitatively theoretical level to analyze the antioxidant behavior. In this work, the micromechanisms of the antioxidant behavior affected by polarity in the olive oil were systematically investigated by experimental and computational methods. The results showed that the polarity of antioxidants decreased with the growth of the alkyl chains, which had multiple impacts on the effectiveness of antioxidants. The excessive polarity gap between the antioxidant and oil molecules would cause the antioxidant to be dispersed at the oil−air interface, which could enhance their antioxidant ability. Meanwhile, the antioxidants with longer alkyl chains had lower polarity and better dispersibility but decreased mobility. Hence, compared with other antioxidants, medium polarity antioxidants presented both good dispersion and relatively suitable migration, indicating that they would have an optimal antioxidant effect.

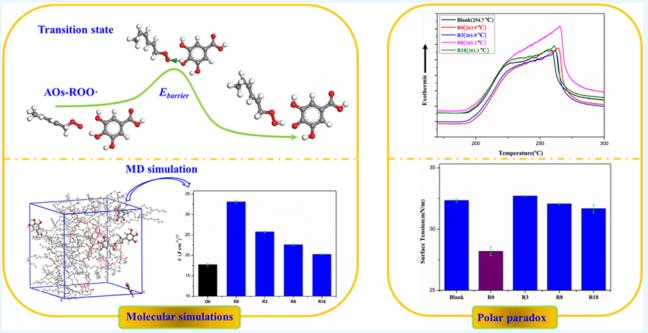

1. INTRODUCTION

Olive oils play a unique role in human life for their nutritional and medicinal properties.[1] However, the polyunsaturated fatty acids present in olive oil are susceptible to oxidation and form active free radicals in the presence of heat, light, reactive oxygen species, metals, etc.[2] Oxidation not only produces rancid odors and flavors but also decreases the nutritional quality and safety by the formation of secondary products.[3] Therefore, it is important to ensure the oxidative stability during processing, handling, and storage without reducing the quality of the oil. Usually, adding qualified synthetic or natural antioxidants (AOs) is one of the effective ways to minimize the oxidation degree of food oil.[4]

Nowadays, for health reasons, researchers' interest is shifted toward natural counterparts rather than synthetic antioxidants.[5] Numerous kinds of natural compounds are available as the antioxidant, such as tocopherols, ascorbic acid, phenolic acids, flavonoids, etc.[6,7] This is also a challenge for researchers to figure out what kind of antioxidants among those huge candidates are optimally suited for protecting different food oils.[8] Lot of researches have proved that the antioxidant effect of AOs can be affected by multiple factors, which include the phenolic hydroxyl group (−O−H) bond dissociation energy (BDE) or steric hindrance,[9] and some physical factors.[10] To be more specific, those physical factors are related to the diffusion, self-aggregation, and location of AOs, which are mainly governed by the molecular polarity. However, the complex influence of polarity on antioxidant effectiveness is still not clear.[11]

Thus, understanding the behavior of AOs affected by polarity in the oil has been a major challenge for current food research,[12] which some progress has been made. Based on the large body of antioxidant effectiveness data generated from the early studies, the polar paradox pointed out that polar antioxidants tend to be more effective than nonpolar antioxidants in the nonpolar media.[13] However, the polar paradox tends to fail in several circumstances. For instance, the capacities of antioxidants in the oil were greatly influenced by their concentration.[14] Also, only when the polar antioxidant reached a certain concentration would the polar paradox be met. As for a complete homologous series of antioxidants and its alkyl esters, there was a nonlinear effect of the alkyl chain of AOs on their antioxidant ability. The antioxidant with medium chain length got the optimal performance, which was named as "cutoff" effect.[15] However, even though scientists have been committed to this field for years, progress was slow for the lack of cognition on the micromechanism, especially from

Received: January 8, 2021
Accepted: February 25, 2021
Published: March 4, 2021

theoretical aspects to reveal the mechanisms of polarity in the antioxidant process of AOs.

Nowadays, with the development of computer science, molecular simulation technology is playing a growing role in academic and industrial research fields.[16] Compared with the conventional experimental method, the molecular simulation is a valuable theoretical approach and may provide a reasonable microlevel quantitative understanding of the mechanisms.[17,18] Through quantum mechanics (QM) simulations, the transition state energy and bond dissociation energy (BDE) could be applied to uncover the chemical reaction mechanism from the energy point of view.[19,20] Moreover, with the help of the molecular dynamic (MD) simulations, many structural physical parameters for materials in the specific system, such as the solubility parameters (δ), mean square displacement (MSD), and interaction energy ($E_{binding}$), can be obtained.[21] For example, the diffusion coefficient (D), solution coefficient (S), solubility parameter (δ), etc. were comprehensively computed for 18 natural antioxidants to build a predictive strategy of screening the effective phenolic antioxidants in rubber composites.[22] Rajan and Muraleedharan used the 6−311++ G (df, p) basis set for analyzing the structures of polyphenol and Gallic acid (GA), and the hydrogen atom transfer and transition metal chelation mechanisms were proved as the preferred mechanisms for GA.[23]

The goal of this work was to strengthen the understanding of the relationship between antioxidant capacity and the polarity of AO molecules and provide a quantitatively theoretical comprehension of the structure−property relationship, which may guide the work in the selection and modification of antioxidants. The antioxidant gallic acid and its alkyl ester derivatives with different polarities, i.e., propyl gallate, octyl gallate, and octadecyl gallate, were selected in the antioxidation studies of olive oil. These four types of AOs were named R0, R3, R8, R18, respectively, according to the length of its alkyl chain (the tail number 0, 3, 8, and 18 indicated the number of carbon atoms of the alkyl ester derivatives). First, the antioxidant effect of AOs was evaluated experimentally. Then, by both experiments and simulations, the antioxidant behavior affected by polarity in the olive oil was investigated in depth according to the computational parameters that included the bond dissociation energy (BDE), the reaction energy barrier, solubility parameter (δ), mean square displacement (MSD), the surface tension, etc.

2. RESULTS AND DISCUSSION

2.1. The Oxidation Degrees in Surface and Internal Sites. Experimentally, the oil sample was put in the air-circulating cabinet oven at 100 °C for 12 h, and the oxidation degrees in surface and internal sites were collected for FT-IR testing. Usually, the aging materials will change their chemical structures after thermo-oxidative aging and generate various functional groups, such as carbonyl, aldehyde, and ethers.[24] As shown in the FT-IR result in Figure 1, after aging for 12 h, the ratio of the carbonyl absorption peak (1730 cm^{-1}) to that of CH_2 (2848 cm^{-1}), denoted as C(C═O)/C(CH2), could reflect the oil oxidation degree.[25] In this study, the value of C(C═O)/C(CH_2) of the surface, internal, and original samples were 2.98, 1.86, and 1.45, respectively. It indicated that the oil sample at the surface had more carbonyl compounds than the internal sample located inside, which meant that the oil on the surface was more susceptible to oxidation.

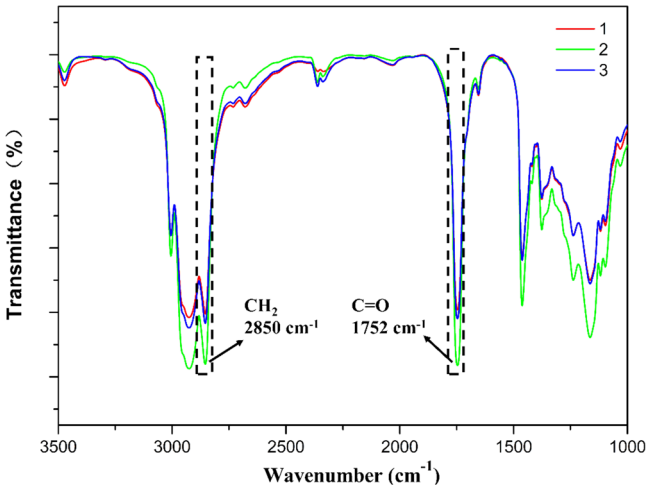

Figure 1. FT-IR spectra for original (1), internal (2), and surface (3) samples.

2.2. DSC Analysis. Figure 2 presents the DSC curves of the blank sample and the oil samples with different antioxidants

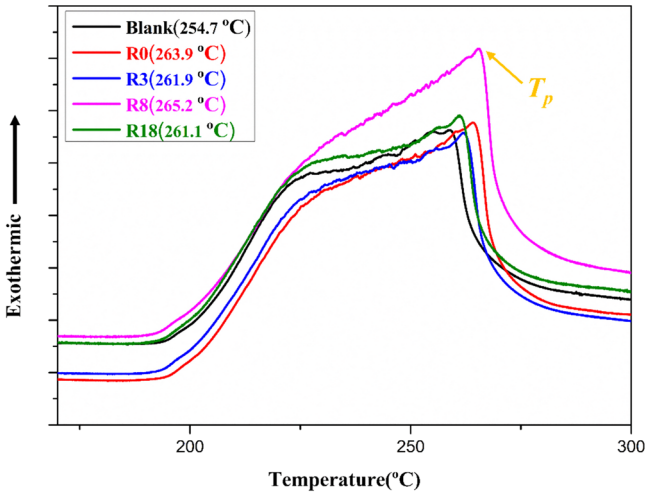

Figure 2. DSC curves of different AO composites under an O_2 atmosphere.

under the O_2 atmosphere. T_p is identified as the temperature when the heat flow has reached a maximum point on the DSC spectra and can be used for the assessment of the oxidative stability.[26] The blank sample manifested a lower T_p than the sample containing antioxidants. Antioxidants with medium polarity (i.e., R8) had the optimal antioxidant effect with a T_p of 265.2 °C. Moreover, the T_p of the oil sample with a polar antioxidant (R0) was higher than that of a less polar antioxidant (R3). The introduction of antioxidants improved the thermo-oxidative aging of oil, and the antioxidant effect ranking of these four antioxidants was R8 > R0 > R3 > R18 according to the T_p values. The antioxidant mechanisms (or behavior) of AOs in the oil may be analyzed through molecular simulation in the following sections.

2.3. Antioxidation Analysis. *2.3.1. Bond Dissociation Energy and the Reaction Energy Barrier.* The bond dissociation energy (BDE) and the reaction energy barrier were calculated according to the section 4.5 methods, and the calculation results were presented in Table 1 and Table 2,

https://dx.doi.org/10.1021/acsomega.1c00120
ACS Omega 2021, 6, 7119−7126

Table 1. Hydrogen Dissociation Enthalpies for Antioxidants and Fatty Acids[a,b,c,d]

dissociation position	1[a]	1[b]	1[c]	1[d]	2	3
ΔG_{298K} (kJ·mol^{-1})	316.2	316.1	315.6	315.2	304.5	345.4

[a]R0. [b]R3. [c]R8. [d]R18.

respectively. The dissociation positions of hydrogen in molecules (the position with the lowest BDE value for different molecules) were indicated in Figure 3. The values of O−H bond dissociation energy of AOs showed no significant difference (located between 315.2−316.2 kJ·mol^{-1}), all were lower than that for the C−H bond in oleic acid (345.4 kJ·mol^{-1}) but slightly higher than the one for linoleic acid (304.5 kJ·mol^{-1}). This indicated that the gradually increasing alkyl chain had little effect on the BDE values of AOs. Also, compared with oleic acid, linoleic acid was more sensitive to oxidation because the C−H bond at position 2 was more prone to dissociation due to its lower BDE value.

Moreover, through the calculated reaction energy barrier, the oxidation and antioxidant protective mechanisms can be analyzed deeply. Since the linoleic acid was more sensitive to oxidation and the limitation of calculation conditions, the structures of RH and ROO· were simplified as shown in Figure 4. As provided in Table 2, the energy barrier between antioxidants and ROO· (2.6−3.4 kJ·mol^{-1}) was much lower than the one of oil and ROO· (49 kJ·mol^{-1}), which meant all of the antioxidants had pretty good antioxidant efficacy. This might be due to the greater steric hindrance that ROO· needed to overcome to capture the hydrogen from RH. In contrast, it was easier to capture hydrogen from AOs. Therefore, in terms of BDE and the reaction energy barrier, all of these antioxidants could give a hydrogen atom to the peroxyl radical ROO· and then terminate the free-radical chain reaction. From the chemical perspective of QM results, it also indicated that each antioxidant should have a consistent antioxidant potential, because the results of the reaction energy barrier and BDE were within the calculation error range. The cause of the inconsistent effects of AOs was more likely to be physical factors, which would be discussed as follows.

2.3.2. Dispersion and Migration of Antioxidants. Besides the above chemical factors, some physical factors of the systems also affect the efficiency of the antioxidant in the oil, especially the dispersion and migration of AOs.[11] During the oxidation process of oil, the positions where the unsaturated fatty acids dissociate to produce free radicals are random. Moreover, antioxidants need to be mobile enough for encountering the oxidation sites and, subsequently, block the spread of unstable free radicals. Therefore, to achieve a better antioxidant effect in the oil, high mobility and good dispersibility in the oil matrix are usually required for AOs.

In fact, with the aid of MD simulation, the solubility parameter can be applied to estimate the compatibility and dispersion of different components. The smaller the absolute value of the solubility parameter difference between AOs and oil, the better compatibility and dispersion of the antioxidant.[27] The solubility parameter (δ) is expressed as the following equation.

$$\delta = \sqrt{\mathrm{CED}} = \sqrt{\frac{E_{\mathrm{coh}}}{V}} = \sqrt{\frac{\Delta H_{\mathrm{vap}} - RT}{V}} \quad (1)$$

where CED means the cohesive energy density; E_{coh} is the cohesive energy; V is the mole volume. ΔH_{vap}, R, and T represent the enthalpy of vaporization, gas constant, and the absolute temperature, respectively.

The calculated solubility parameters of antioxidants and oil are present in Figure 5. The solubility parameters of antioxidants declined from R0 to R18 as the length of the alkyl chain became longer. The difference in solubility parameter values between the nonpolar antioxidants (R8 and R18) with oil was small, which meant they might achieve better dispersion in the oil matrix. However, R0 and R3 systems were just the opposite which could weaken their protective efficiency.

Furthermore, to investigate the migration of the antioxidant in oil quantifiably, the mean square displacement (*MSD*) was employed, which was defined by the following equation.[28]

$$\mathrm{MSD} = \frac{1}{N}\sum_{i=1}^{N}\langle |r_i(0) - r_i(t)|^2 \rangle \quad (2)$$

where the $r_i(0)$ and $r_i(t)$ represent the initial position of atom i and the position after a period of time t. $|r_i(0)-r_i(t)|$ is the displacement of atom i in time t. N is the total number of atoms in the selected antioxidant molecules, and the angle brackets, $\langle\ \rangle$, indicates the average value of the square of displacement for atom i.

Among all antioxidants, R0 had the highest *MSD* values, followed by R3, R8, and R18, which meant that the increasingly long alkyl chain reduced the mobility of antioxidants (Figure 6c). This might be due to the fact that increasing the molecular weight of AOs brought about the difficulty of the molecular movement. The interaction of the antioxidant molecule with the oil was then enhanced, which would be confirmed in the following result of E_{binding}. Some antioxidants, such as R0 and R3, would form aggregates in the oil due to the large polarity difference. The hydrogen bonds were found between the agglomerated antioxidant molecules (Figure 6b), which hindered the movement of the molecules and reduced their *MSD* values (Figure 6d).

The E_{binding} values were calculated using eq 3, and here, the R0/oil system is taken as an example.

$$E_{\mathrm{binding}} = -E_{\mathrm{inter}} = -(E_{\mathrm{total}} - E_{\mathrm{R0}} - E_{\mathrm{oil}}) \quad (3)$$

where E_{total} is the energy of the total system. E_{R0} and E_{oil} represent the energies of R0 and oil, respectively. In fact, the higher the E_{binding} values are, the stronger the nonbonding interactions between molecules are.[29] The calculation results of E_{binding} are shown in Figure 7.

As expected, the antioxidants with longer alkyl chains, i.e., the R18 system, got the higher E_{binding} value. In fact, in order to

Table 2. Energy Barrier of the Reaction of Antioxidants (or RH) with Peroxyl Radical ROO·

transition states	R0−ROO·	R3−ROO·	R8−ROO·	R18−ROO·	RH−ROO·
E_{barrier} (kJ·mol^{-1})	3.4	2.9	2.6	2.8	49.0
imaginary frequency (cm^{-1})	−1042.7	−1125.6	−1181.1	−1176.1	−1396.6

https://dx.doi.org/10.1021/acsomega.1c00120
ACS Omega 2021, 6, 7119−7126

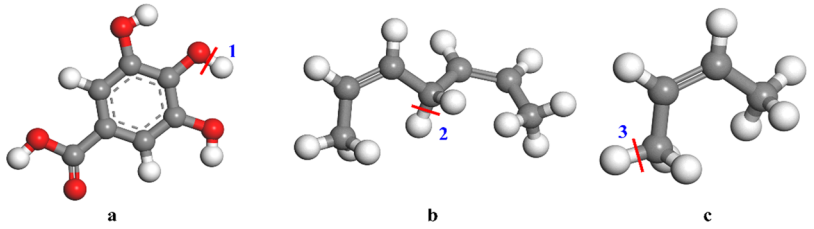

Figure 3. Dissociation positions of hydrogen in antioxidants (a), fatty acids (linoleic acid) (b), and oleic acid (c). (White, red, and gray spheres represent H, O, and C atoms, respectively.).

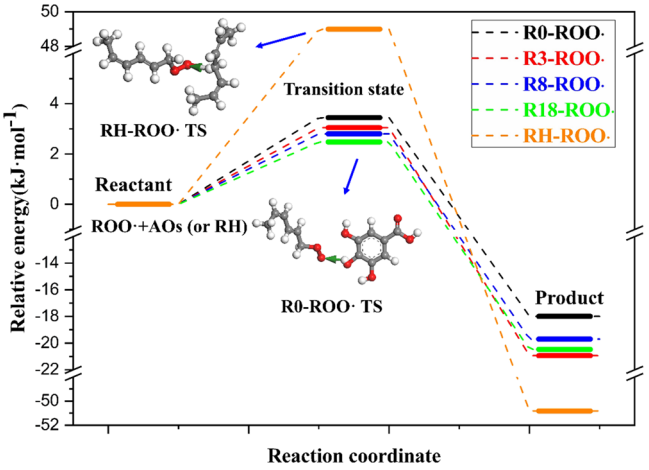

Figure 4. Energy barrier of reaction and transition states (TS) for AOs (or RH) with a peroxyl radical. (White, red, and gray spheres represent H, O, and C atoms, respectively. In addition, the three-dimensional green arrow in transition states represents the vibration mode of the atom.).

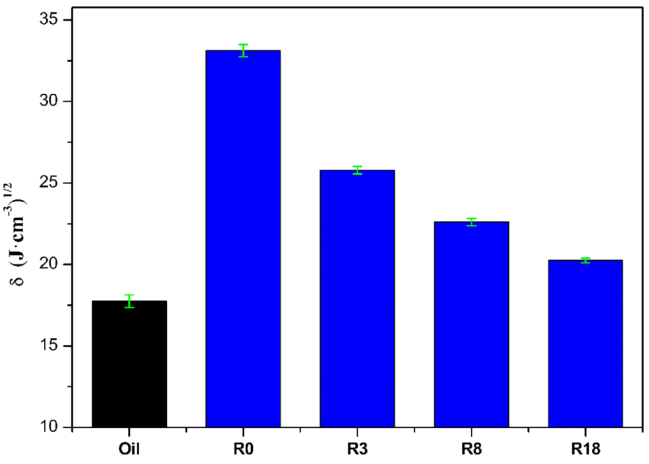

Figure 5. Solubility parameters for antioxidants and oil.

achieve better dispersion, the binding energy between the antioxidant and the oil molecules needed to be greater than the energy between itself. However, the $E_{binding}$ value between the polar antioxidant (R0 and R3) and the oil was less than (or close to) the $E_{binding}$ value of the antioxidant. Thus, R0 and R3 were more likely to form agglomeration in the oil if compared with R8 and R18 systems. In contrast, R8 and R18 could achieve better dispersion in oil. Therefore, the medium polarity antioxidant R8 got optimal performance in the oil for the combination of better dispersion and higher mobility, and this could be the microscopic reason for the "cutoff" effect.

Moreover, due to the large gap of polarity parameters between the polar antioxidant and oil, the distribution of those antioxidants in the oil might be different from the nonpolar antioxidant. Some antioxidants could be located at the oil−air interface.[30] That would change the surface tension of the oil. Figure 8 shows the surface tension of oil with different antioxidants. The surface tension of the R0 system decreased, but the surface tension of the other antioxidant systems did not change significantly. This proved that the R0 molecules might be distributed on the oil−air interface. Since the oil−air interface was one of the important sites where oil oxidation occurs, as indicated by the experimental results in section 2.1, the distribution of R0 at the interface would be beneficial to improve its antioxidant effect.

2.3.3. Analysis of Oxygen Permeability. Oxygen is the key participant during the course of oil oxidation, and it will react with an alkyl radical to form a peroxyl radical. To explore the influence of R0 molecules located at the air−oil interface on the O_2 barrier of oil, according to the sorption-solution-diffusion progress of gas permeability, the gas permeability coefficient P can be defined as follows:[31]

$$P = D \times S \tag{4}$$

Here, D and S are the diffusion coefficient and solution coefficient, respectively. The solution coefficient S was investigated by the adsorption isotherm over a range of pressure from 0 to 1 atm at 298 K. Then, the S of oxygen can be acquired from the slope of the adsorption isotherm plot when the pressure approaches a limit of 0 kPa as the following equation shows:

$$S = \lim_{p\to 0}\left(\frac{C}{p}\right) \tag{5}$$

where C is the adsorption concentration of O_2 in oil [$cm^3(STP)/cm^{-3}$], and p is pressure (Pa).

The diffusion coefficient D of oxygen was computed from eq 6 based on the Einstein−Smoluchowski equation.

$$D = \frac{1}{6N}\lim_{t\to\infty}\frac{d}{dt}\sum_{i=1}^{N}\langle |r_i(0) - r_i(t)|^2\rangle \tag{6}$$

In the expression, N is the total number of diffusing atoms i. Also, $r_i(0)$ and $r_i(t)$ are the initial and final position vectors of diffusing atoms i over the time interval t. $\langle |r_i(t)-r_i(0)|^2\rangle$ represents ensemble averages of the *MSD* of the inserted gas molecule trajectories.

The P, D, and S values for O_2 in oil and R0/oil systems at 298 K are listed in Table 3. It was evident that the R0/oil system had a lower permeability coefficient (0.5×10^{-9} $cm^2 \cdot s^{-1} \cdot kPa^{-1}$) than the oil system ($3.9 \times 10^{-9}$ $cm^2 \cdot s^{-1} \cdot kPa^{-1}$) at the same temperature, implying that the enrichment of R0

https://dx.doi.org/10.1021/acsomega.1c00120
ACS Omega 2021, 6, 7119−7126

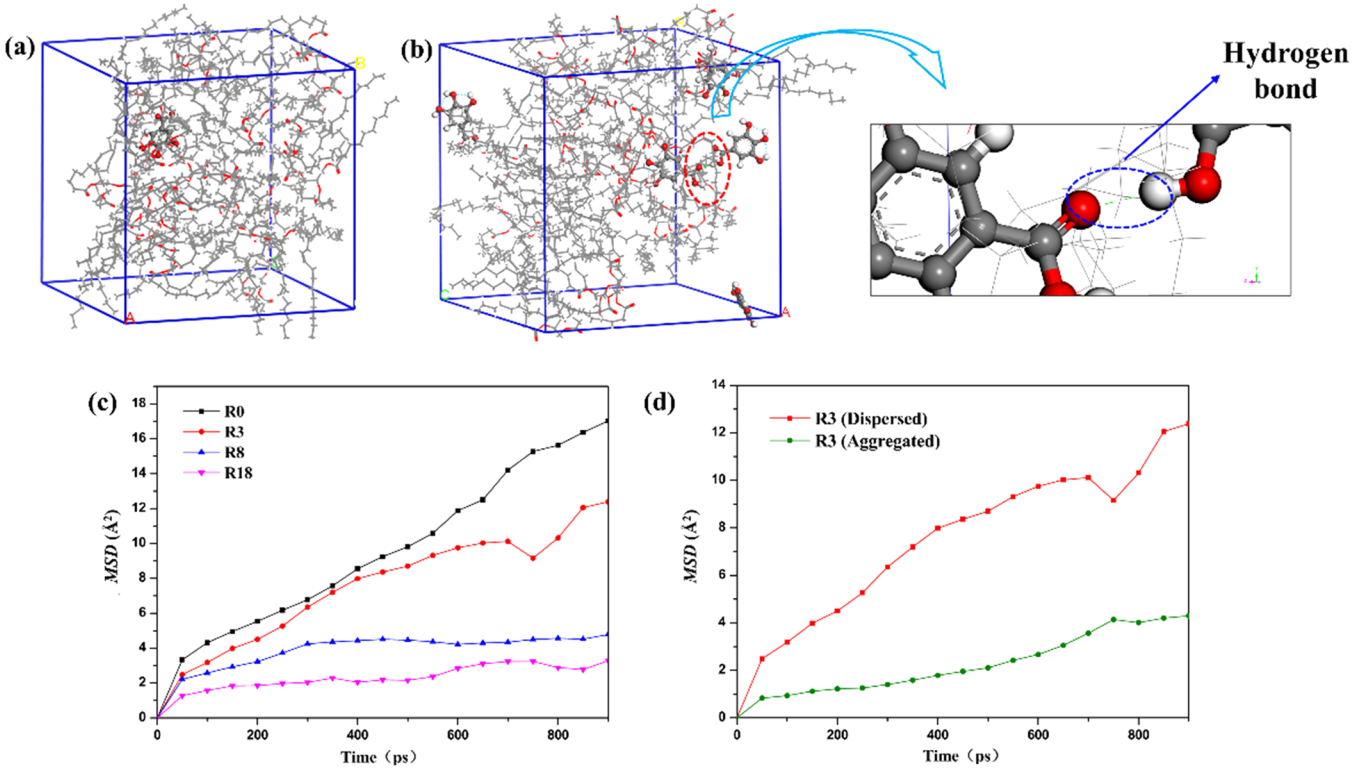

Figure 6. Amorphous cells for R0/oil at a ratio of 1:20 (a) and 5:20 (b). (White, red, and gray spheres or lines represent H, O, and C atoms, respectively.) (c) and (d) are the *MSD* curves of antioxidants in the oil.

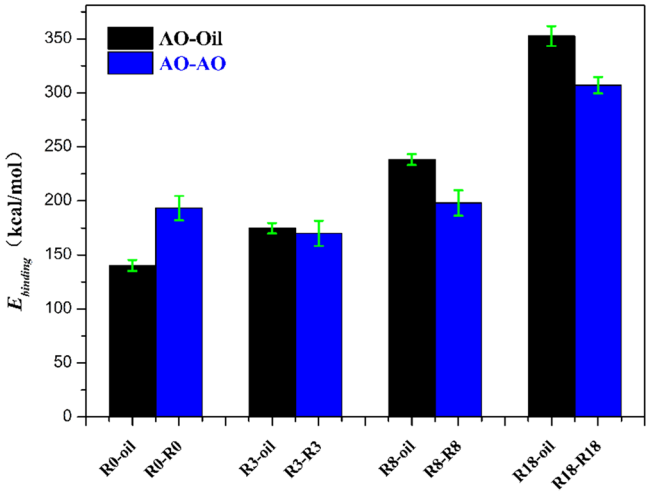

Figure 7. $E_{binding}$ between different materials.

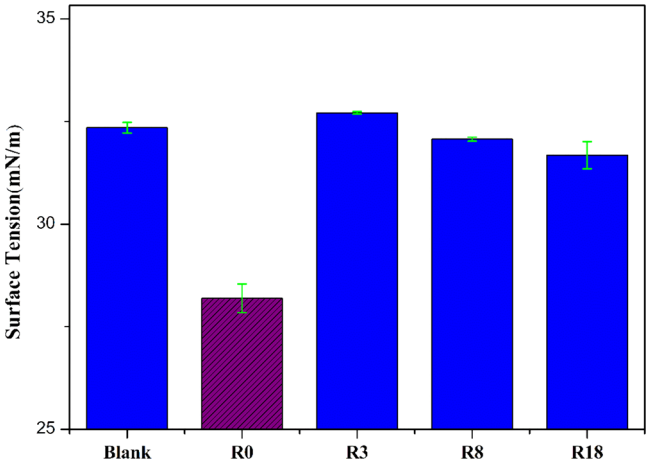

Figure 8. Surface tension of oil with or without antioxidants.

molecules would affect the permeability of O_2 into the oil matrix. Combining the results of surface tension and the permeability coefficient, it can be concluded that the R0 molecules distributed at the oil−air interface will block the entry of oxygen, which may also be one of the reasons for the polar paradox phenomenon.

3. CONCLUSIONS

In this work, the micromechanism of polarity that affected the efficacy of antioxidants in olive oil was studied through the combination of experiments and molecular simulations. The main conclusions were summarized as follows:

Table 3. *D*, *S*, and *P* Values for O_2 in Oil and R0/Oil Systems at 298 K

systems	D ($\times 10^{-6}$ $cm^2 \cdot s^{-1}$)	S ($\times 10^{-4}$ $cm^3(STP) \cdot cm^{-3}$)	$P = D \times S$ ($\times 10^{-9}$ $cm^2 \cdot s^{-1} \cdot kPa^{-1}$)
oil	2.3 ± 0.5	16.9 ± 2.4	3.9
R0/oil	1.5 ± 0.4	3.2 ± 0.2	0.5

(1) Among Gallic acid and its ester series, the oil with medium chain length antioxidant R8 exhibited the optimal thermo-oxidative stability. The polar antioxidant R0 had better antioxidant efficiency than its less polar derivative R3.

(2) The gradual growth of the alkyl chain reduced the polarity of antioxidants, and nonpolar antioxidants (R8

https://dx.doi.org/10.1021/acsomega.1c00120
ACS Omega 2021, 6, 7119−7126

and R18) had better dispersion in the oil. However, the polar antioxidants (R0 and R3) were easy to form agglomeration in the oil, which would affect their dispersion performance. However, the oversized alkyl segments would hinder the diffusion of antioxidant molecules. As a result, the medium-polarity antioxidant could achieve a better balance of dispersion and mobility, which might be the reason for the "cut off" effect.

(3) Due to the excessively large polarity gap, R0 and oil were mutually repulsive, so that R0 would be distributed at the oil−air interface, the place where oil is prone to oxidation. However, the R0 molecule at the oil−air interface hindered the permeation of oxygen into the oil matrix. All of that would enhance the antioxidant effect of polar antioxidant R0, which might be the microscopic reasons of the polar paradox.

In conclusion, the effect of polarity on the performance of antioxidants is multifaceted. The polarity will affect the dispersion, as well as the migration of antioxidants in the oil. Given these effects, R0 and R8 may have a synergistic interaction. This is because R0 molecules can accumulate at the oil−air interface and block the entry of oxygen, while R8 exerts a good antioxidation effect inside the oil, and the related research will be carried out in the follow-up work.

4. MATERIALS AND METHODS

4.1. Materials. Extra virgin olive oil was bought from Aceites Abril SL, Spain. Methanol (≥99%) and ethanol (≥99%) were supplied by Beijing Chemical Works. Also, *n*-hexane (≥97%) was purchased from Shanghai Aladdin Biochemical Technology Co., Ltd. As for the antioxidants, gallic acid (≥99%) was purchased from J&K Scientific Ltd. Propyl gallate (≥98%) was provided by Beijing Minruida Technology Co., Ltd. Octyl gallate (≥98%) was obtained from Shanghai Yuanye Biological Technology Co., Ltd. The molecular structures of AOs are presented in Figure 9.

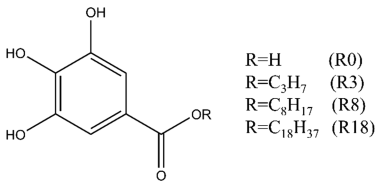

Figure 9. Molecular structures of antioxidants with different alkyl chain lengths.

The preparation of the testing sample was as follows. Different antioxidants were solubilized in ethanol, and 20 μL of the solution was added in olive oil to obtain the desired concentration of 100 M. Then, the dry nitrogen was passed into the oil for 10 min and sonicated for 15 min to remove the ethanol.

4.2. DSC. The thermodynamic performance was conducted on the differential scanning calorimeter (DSC) (NETZSCH, Germany) under the oxygen atmosphere from room temperature to 300 °C at a heating rate of 10 °C/min.[32]

4.3. Fourier Transform Infrared Spectroscopy (FT-IR). FT-IR spectra were measured with an FT-IR spectrometer (VERTEX 70, Germany) in the middle IR region (4000−1000 cm^{-1}) at a resolution of 4 cm^{-1}. The KBr pressed disk technique was used.

4.4. Surface Tension. The pendant drop method was applied for the surface tension test and was carried on a contact angle meter (Dataphysics, Germany). First, a sufficiently large droplet was injected with a blunt-end metal needle. To make the droplet reach equilibration, the drop image was acquired by the digital camera after 5 s. Then, the surface tension was calculated by software that came with the instrument according to the Young−Laplace equation as following.[33]

$$\Delta P = \gamma\left(\frac{1}{R_1} + \frac{1}{R_2}\right) \tag{7}$$

Here, ΔP is the pressure difference between the interfaces, γ is the surface tension, and R_1 and R_2 are the main radii of the curvature of the droplets.

4.5. Quantum Mechanics Simulation. The hydrogen atom transfer (HAT) process is one of the major antioxidative mechanisms for an antioxidant (AH). AH can provide a hydrogen atom (H·) for the peroxyl radical (ROO·) to convert it to ROOH and then significantly delay the oxidation of the oil.[34] Therefore, the bond dissociation energy (BDE) of the dissociation reaction for active hydrogen atoms in the antioxidant can reflect its antioxidant capacity.[35] Moreover, for a specific chemical process, there generally exists the energy of a transition state (TS), which can be regarded as a barrier to be overcome for a reaction occurrence. The lower BDE and the transition state energy barrier means the stronger the ability of antioxidant molecules to capture the free radicals.[36]

For quantum mechanics (QM) simulation, the calculation work was based on the first-principles density functional theory by the Dmol3 module in Materials Studio (MS) suite software. The Kohn−Sham equation was applied to calculate the multiparticle system's potential. As for the exchange−correlation potential, the generalized gradient approximation (GGA) with the Perdew−Burke−Ernzerhof (PBE) function was employed. The triple numerical plus polarization (TNP) was selected as the atomic orbital basis set. Also, the multiplicity for the free radical was used as doublet with the spin unrestricted. The self-consistent field (SCF) procedure was applied, and its convergence tolerance was set to 10^{-6} au for a fine convergence quality criterion.

All molecule structures needed to be optimized at first. While implementing the geometry optimization, the convergence threshold of displacement was 0.005 Å, the maximum allowable force was 0.002 Hartree/Å, and the convergence threshold of energy was 10^{-5} au. The specific thermodynamic cycle, taking R0 as an example, is illustrated schematically in Figure 10. The energy E (for AH, A·, or H·) was the electronic energy at 0 K and obtained after geometry optimization. As for the hydrogen dissociation energy ΔG^T at a certain temperature

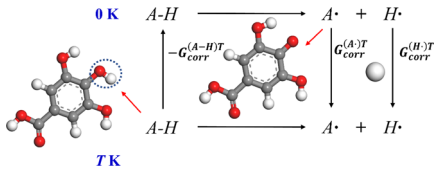

Figure 10. Example of the thermodynamic cycle for R0 in the DMol3. (White, red, and gray spheres represent hydrogen, oxygen, and carbon atoms, respectively).

https://dx.doi.org/10.1021/acsomega.1c00120
ACS Omega 2021, 6, 7119−7126

(T), it can be obtained from eq 8 (with antioxidant AH as an example).

$$\Delta G^{T} = [E(\mathrm{A}\cdot) + G_{\mathrm{corr}}^{(\mathrm{A}\cdot)T}] + [E(\mathrm{H}\cdot) + G_{\mathrm{corr}}^{(\mathrm{H}\cdot)T}] - [E(\mathrm{AH}) + G_{\mathrm{corr}}^{(\mathrm{AH})T}] \quad (8)$$

Here, $E(\mathrm{A}\cdot)$, $E(\mathrm{H}\cdot)$, $E(\mathrm{AH})$ represented the energy of A·, H·, and AH at 0 K, respectively. GT corr is the thermodynamic correction of the corresponding structures at a certain temperature (T).

As for the calculation of the reaction energy barrier, the complete linear synchronous transit/quadratic synchronous transit (complete LST/QST) method was used to acquire the minimum energy pathway from the reactant to the product.[37] The reasonable structure and vibration mode that could represent the ultimate transition state should only have one imaginary frequency.[38]

4.6. Molecular Dynamics Simulation. Molecular dynamics (MD) simulation is a powerful tool to explore the location and mobility of molecules in the composite system intuitively and quantitatively, through some parameters such as the solubility coefficients (δ), mean square displacement (MSD), etc.[39] To further understand how the polarity of AOs affects its performance, AO (including R0, R3, R8, and R18)/oil amorphous cell models were built. The structure of triacylglycerol for olive oil may be simplified as monounsaturated triacylglycerols, OOO (O, oleic acid), according to the main fatty acid composition of the olive oil.[40] Then, all the MD simulations were performed with the condensed-phase optimized molecular potentials for atomistic simulation studies (COMPASS) force field. The pressure and temperature were controlled by Andersen barostat and Noes thermoset methods, respectively. As for the electrostatic interactions, the Ewald summation method was employed to ensure the accuracy of 0.001 kcal·mol^{-1}. The van der Waals interactions were calculated by using the Lennard−Jones function with a cutoff distance of 12.5 Å. The Newtonian motion equation was integrated by a Verlet velocity time integration algorithm with a time step of 1 fs. The cells containing oil and antioxidant molecules were built through the amorphous cell. After the cells were built, a series of simulation procedures was performed to ensure each cell get to thermodynamic equilibrium by running the Forcite module work. First, a geometry optimization task was applied on the original building cells. Then, the cells underwent an anneal task from 300 to 500 K with 50 annealing cycles by an NVE ensemble (constant number of atoms, constant volume, and constant energy). The annealed cells were further relaxed through 500 ps of NVT ensemble (constant number of atoms, constant volume, and constant temperature) and 1000 ps of NPT ensemble (constant number of atoms, constant pressure, and constant temperature) dynamic simulations. Finally, the related physical parameters can be calculated from the completely equilibrium cell.

AUTHOR INFORMATION

Corresponding Authors

Bianying Wen − *Beijing Key Laboratory of Quality Evaluation Technology for Hygiene and Safety of Plastics, Beijing Technology and Business University, Beijing 100048, PR China*; Email: wenby@btbu.edu.cn

Sizhu Wu − *State Key Laboratory of Organic−Inorganic Composites, Beijing University of Chemical Technology, Beijing 100029, PR China*; orcid.org/0000-0001-7863-2954; Email: wusz@mail.buct.edu.cn

Authors

Jie Tang − *State Key Laboratory of Organic−Inorganic Composites, Beijing University of Chemical Technology, Beijing 100029, PR China*

Guohua You − *College of Information Science & Technology, Beijing University of Chemical Technology, Beijing 100029, PR China*

Lu Ruan − *State Key Laboratory of Organic−Inorganic Composites, Beijing University of Chemical Technology, Beijing 100029, PR China*

Yi Lu − *State Key Laboratory of Organic−Inorganic Composites, Beijing University of Chemical Technology, Beijing 100029, PR China*

Complete contact information is available at: https://pubs.acs.org/10.1021/acsomega.1c00120

Notes

The authors declare no competing financial interest.

ACKNOWLEDGMENTS

This work was supported by the National Natural Science Foundation of China (grant no. 51873017), and the Beijing Key Laboratory of Quality Evaluation Technology for Hygiene and Safety of Plastics (grant no. QETHSP2020004).

REFERENCES

(1) Foscolou, A.; Critselis, E.; Panagiotakos, D. Olive oil consumption and human health: A narrative review. *Maturitas.* **2018**, *118*, 60−66.

(2) Choe, E.; Min, D. B. Mechanisms and factors for edible oil oxidation. *Compr. Rev. Food Sci. Food Saf.* **2006**, *5*, 169−186.

(3) Guillén, M. D.; Goicoechea, E. Detection of primary and secondary oxidation products by Fourier transform infrared spectroscopy (FTIR) and 1H nuclear magnetic resonance (NMR) in sunflower oil during storage. *J. Agric. Food Chem.* **2007**, *55*, 10729−10736.

(4) Shahidi, F.; Zhong, Y. Lipid oxidation and improving the oxidative stability. *Chem. Soc. Rev.* **2010**, *39*, 4067−4079.

(5) Berdahl, D.; Nahas, R.; Barren, J. Synthetic and natural antioxidant additives in food stabilization: current applications and future research. In *Oxidation in foods and beverages and antioxidant applications*, 1st ed.; Eric, A. D., Ed.; Woodhead Publishing: Cambridge, 2010; pp. 272−320.

(6) Rokosik, E.; Siger, A.; Rudzińska, M.; Dwiecki, K. Antioxidant activity and synergism of canolol and α-tocopherol in rapeseed oil is affected by the presence of phospholipid association colloids. *LWT.* **2020**, *133*, 110095.

(7) Huang, J.; Sun, Q.; Song, G.; Qi, S.; Chen, J.; Zhang, P.; Geng, T.; Lin, Q.; Duan, Y. Antioxidant and anti-isomerization effects of sesamol and resveratrol on high oleic acid peanut oil. *LWT.* **2020**, *123*, 109077.

(8) Zhong, Y.; Shahidi, F. Antioxidant behavior in bulk oil: limitations of polar paradox theory. *J. Agric. Food Chem.* **2012**, *60*, 4−6.

(9) Guitard, R.; Paul, J. F.; Nardello-Rataj, V.; Aubry, J. M. Myricetin, rosmarinic and carnosic acids as superior natural antioxidant alternatives to α-tocopherol for the preservation of omega-3 oils. *Food Chem.* **2016**, *213*, 284−295.

(10) Laguerre, M.; Lecomte, J.; Villeneuve, P. The use and effectiveness of antioxidants in lipids preservation. In *Handbook of Antioxidants for Food Preservation*; Fereidoon, S., Ed.; Woodhead Publishing: Cambridge, 2015; pp. 349−372.

(11) Laguerre, M.; Bayrasy, C.; Panya, A.; Weiss, J.; McClements, D. J.; Lecomte, J.; Decker, E. A.; Villeneuve, P. What makes good antioxidants in lipid-based systems? The next theories beyond the polar paradox. *Crit. Rev. Food Sci. Nutr.* **2015**, *55*, 183−201.
(12) Poyato, C.; Navarro-Blasco, I.; Calvo, M. I.; Cavero, R. Y.; Astiasarán, I.; Ansorena, D. Oxidative stability of O/W and W/O/W emulsions: Effect of lipid composition and antioxidant polarity. *Food Res. Int.* **2013**, *51*, 132−140.
(13) Porter, W. L.; Black, E. D.; Drolet, A. M. Use of polyamide oxidative fluorescence test on lipid emulsions: contrast in relative effectiveness of antioxidants in bulk versus dispersed systems. *J. Agric. Food Chem.* **1989**, *37*, 615−624.
(14) Shahidi, F.; Zhong, Y. Revisiting the polar paradox theory: a critical overview. *J. Agric. Food Chem.* **2011**, *59*, 3499−3504.
(15) Laguerre, M.; Giraldo, L. J. L.; Lecomte, J.; Figueroa-Espinoza, M. C.; Baréa, B.; Weiss, J.; Decker, E. A.; Villeneuve, P. Chain length affects antioxidant properties of chlorogenate esters in emulsion: the cutoff theory behind the polar paradox. *J. Agric. Food Chem.* **2009**, *57*, 11335−11342.
(16) Dai, T.; Li, R.; Liu, C.; Liu, W.; Li, T.; Chen, J.; Kharat, M.; McClements, D. J. Effect of rice glutelin-resveratrol interactions on the formation and stability of emulsions: A multiphotonic spectroscopy and molecular docking study. *Food Hydrocolloids* **2019**, *97*, 105234.
(17) Thakre, N.; Palodkar, A. V.; Dongre, H. J.; Jana, A. K. Microscopic Molecular Insights Into Hydrate Formation and Growth in Pure and Saline Water Environments. *J. Phys. Chem. A.* **2020**, 4241.
(18) Bay, M. V.; Nam, P. C.; Quang, D. T.; Mechler, A.; Hien, N. K.; Hoa, N. T.; Vo, Q. V. Theoretical Study on the Antioxidant Activity of Natural Depsidones. *ACS Omega* **2020**, *5*, 7895−7902.
(19) Arafet, K.; González, F. V.; Moliner, V. Quantum mechanics/molecular mechanics studies of the mechanism of cysteine proteases inhibition by dipeptidyl nitroalkenes. *Chem. − Eur. J.* **2020**, *26*, 2002−2012.
(20) Vo, Q. V.; Nam, P. C.; Thong, N. M.; Trung, N. T.; Phan, C.-T. D.; Mechler, A. Antioxidant motifs in flavonoids: O−h versus c−h bond dissociation. *ACS Omega* **2019**, *4*, 8935−8942.
(21) Khuntawee, W.; Sutthibutpong, T.; Phongphanphanee, S.; Karttunen, M.; Wong-ekkabut, J. Molecular dynamics study of natural rubber−fullerene composites: connecting microscopic properties to macroscopic behavior. *Phys. Chem. Chem. Phys.* **2019**, *21*, 19403−19413.
(22) Lu, L.; Luo, K.; Yang, W.; Zhang, S.; Wang, W.; Xu, H.; Wu, S. Insight into the anti-aging mechanisms of natural phenolic antioxidants in natural rubber composites using a screening strategy based on molecular simulation. *RSC Adv.* **2020**, *10*, 21318−21327.
(23) Rajan, V. K.; Muraleedharan, K. A computational investigation on the structure, global parameters and antioxidant capacity of a polyphenol, Gallic acid. *Food Chem.* **2017**, *220*, 93−99.
(24) Lazzari, M.; Chiantore, O. Drying and oxidative degradation of linseed oil. *Polym. Degrad. Stab.* **1999**, *65*, 303−313.
(25) Vlachos, N.; Skopelitis, Y.; Psaroudaki, M.; Konstantinidou, V.; Chatzilazarou, A.; Tegou, E. Applications of Fourier transform-infrared spectroscopy to edible oils. *Anal. Chim. Acta* **2006**, *573*, 459−465.
(26) Kowalski, B.; Ratusz, K.; Kowalska, D.; Bekas, W. Determination of the oxidative stability of vegetable oils by differential scanning calorimetry and Rancimat measurements. *Eur. J. Lipid Sci. Technol.* **2004**, *106*, 165−169.
(27) Liu, B. S.; Sun, H.; Wang, J. K.; Yin, Q. X. Solubility of disodium 5′-guanylate heptahydrate in aqueous methanol mixtures. *Food Chem.* **2011**, *128*, 218−221.
(28) Michalet, X. Mean square displacement analysis of single-particle trajectories with localization error: Brownian motion in an isotropic medium. *Phys. Rev. E.* **2010**, *82*, No. 041914.
(29) Du, D.; Tang, Y.; Yang, L.; Tang, C. Effects of Different Grafting Density of Amino Silane Coupling Agents on Thermomechanical Properties of Cross-Linked Epoxy Resin. *Polymer* **2020**, *12*, 1662.
(30) Di Mattia, C. D.; Sacchetti, G.; Mastrocola, D.; Pittia, P. Effect of phenolic antioxidants on the dispersion state and chemical stability of olive oil O/W emulsions. *Food Res. Int.* **2009**, *42*, 1163−1170.
(31) Zheng, W.; Wu, Y.; Yang, W.; Zhang, Z.; Zhang, L.; Wu, S. A Combined Experimental and Molecular Simulation Study of Factors Influencing the Selection of Antioxidants in Butadiene Rubber. *J. Phys. Chem. B* **2017**, *121*, 1413−1425.
(32) Qi, B.; Zhang, Q.; Sui, X.; Wang, Z.; Li, Y.; Jiang, L. Differential scanning calorimetry study–assessing the influence of composition of vegetable oils on oxidation. *Food Chem.* **2016**, *194*, 601−607.
(33) Khan, H.; Seddon, J. M.; Law, R. V.; Brooks, N. J.; Robles, E.; Cabral, J. T.; Ces, O. Effect of glycerol with sodium chloride on the Krafft point of sodium dodecyl sulfate using surface tension. *J. Colloid Interface Sci.* **2019**, *538*, 75−82.
(34) Ingold, K. U.; Pratt, D. A. Advances in radical-trapping antioxidant chemistry in the 21st century: a kinetics and mechanisms perspective. *Chem. Rev.* **2014**, *114*, 9022−9046.
(35) Galano, A.; Mazzone, G.; Alvarez-Diduk, R.; Marino, T.; Alvarez-Idaboy, J. R.; Russo, N. Food Antioxidants: Chemical Insights at the Molecular Level. *Annu. Rev. Food Sci. Technol.* **2016**, *7*, 335−352.
(36) Kaim, A.; Megiel, E. Transition structures and reaction barriers in the styrene−acrylonitrile copolymerization system according to quantum mechanical calculations. *J. Polym. Sci., Part A: Polym. Chem.* **2005**, *43*, 1827−1844.
(37) Kwon, S. H.; Lee, I.; Park, H.; Lee, S. G. Decomposition mechanisms of self-polishing copolymers for antifouling coating materials through first-principles approach. *Prog. Org. Coat.* **2020**, *138*, 105406.
(38) Jiang, Q. G.; Ao, Z. M.; Chu, D. W.; Jiang, Q. Reversible transition of graphene from hydrophobic to hydrophilic in the presence of an electric field. *J. Phys. Chem. C* **2012**, *116*, 19321−19326.
(39) Amaro, M.; Filipe, H. A. L.; Ramalho, J. P. P.; Hof, M.; Loura, L. M. S. Fluorescence of nitrobenzoxadiazole (NBD)-labeled lipids in model membranes is connected not to lipid mobility but to probe location. *Phys. Chem. Chem. Phys.* **2016**, *18*, 7042−7054.
(40) Maggio, R. M.; Kaufman, T. S.; Carlo, M. D.; Cerretani, L.; Bendini, A.; Cichelli, A.; Compagnone, D. Monitoring of fatty acid composition in virgin olive oil by Fourier transformed infrared spectroscopy coupled with partial least squares. *Food Chem.* **2009**, *114*, 1549−1554.

https://dx.doi.org/10.1021/acsomega.1c00120
ACS Omega 2021, 6, 7119−7126